Isomeric Ratios in Several Inverse (γ, n) and (n, γ) Reactions

Bui Minh Hue[1,2,*] and Tran Duc Thiep[1,2]

[1]*Graduate University of Science and Technology, VAST, 18 Hoang Quoc Viet, Hanoi*

[2]*Institute of Physics, VAST, 10 Dao Tan St., Ba Dinh Region, Hanoi, Vietnam*

bmhue@iop.vast.ac.vn

We measured isomeric ratios of ^{137m,g}Ce, ^{115m,g}Cd, ^{109m,g}Pd, and ^{81m,g}Se produced by 25 MeV bremsstrahlung and thermal neutron induced reactions, namely from inverse (γ, n) and (n, γ) reactions. The bremsstrahlung and the neutron sources were constructed at the electron accelerator Microtron MT-25 of the FLNR, JINR, Dubna, Russia. The activation method combining with off-line gamma-ray spectroscopy was used in the experiment. To improve the accuracy of the isomeric ratio determination, data analysis and necessary corrections, such as the self-absorption and summing cascade effects, were made in gamma rays radioactivity measurements. The results were discussed and compared with those in the existing literature. The obtained results in the (γ, n) reactions were validated by comparison with the theoretical predictions using TALYS 1.95 code.

1. Introduction

The inverse nuclear reactions, when a projectile of one reaction is the ejectile of another reaction, have been subjects for many experimental and theoretical studies since 1960s [1,2]. Inverse reactions including photonuclear and thermal neutron capture reactions play an important role in astrophysics and the study of nuclear structure and nuclear reaction mechanisms [2–4]. So far, most investigations about photonuclear reaction and thermal neutron capture reactions have concentrated on the determination of reaction cross section or reaction yield, but the studies on isomeric ratio (IR) have been still limited. The isomeric ratio, the ratio of the probability for forming isomeric and ground states, provides diverse information about the nuclear structure and nuclear reaction mechanism [5–8]. This ratio is connected with many problems of modern nuclear physics and can be used to test different models of nuclear reactions induced by various projectiles.

The aim of this work was to investigate IR of ^{137m,g}Ce, ^{115m,g}Cd, ^{109m,g}Pd, and ^{81m,g}Se produced in inverse (γ,n) and (n,γ) reactions by activation method, namely ^{138}Ce(γ,n)^{137m,g}Ce, ^{136}Ce(n,γ)^{137m,g}Ce, ^{116}Cd(γ,n)^{115m,g}Cd, ^{114}Cd(n,γ)^{115m,g}Cd,^{110}Pd(γ,n)^{109m,g}Pd, ^{108}Pd(n,γ)^{109m,g}Pd, ^{82}Se(γ,n)^{81m,g}Se, and ^{80}Se(n,γ)^{81m,g}Se. The experimental results are expected to examine the role of the reaction channel effect, intake momentum and impulse effects on the IRs. Moreover, the obtained results in the (γ,n) reactions were compared with the theoretical predictions using TALYS 1.95 code.

2. Experimental procedure

The bremsstrahlung source is obtained by interaction of 25 MeV electron beam produced from MT-25 Microtron accelerator [9] and a 3 mm thickness W disk detailed in

refs. [7,10]. The end-point energy of bremsstrahlung is 25 MeV. The bremsstrahlung spectra, which were simulated by GEANT4 toolkit [11], are shown on Fig.1.

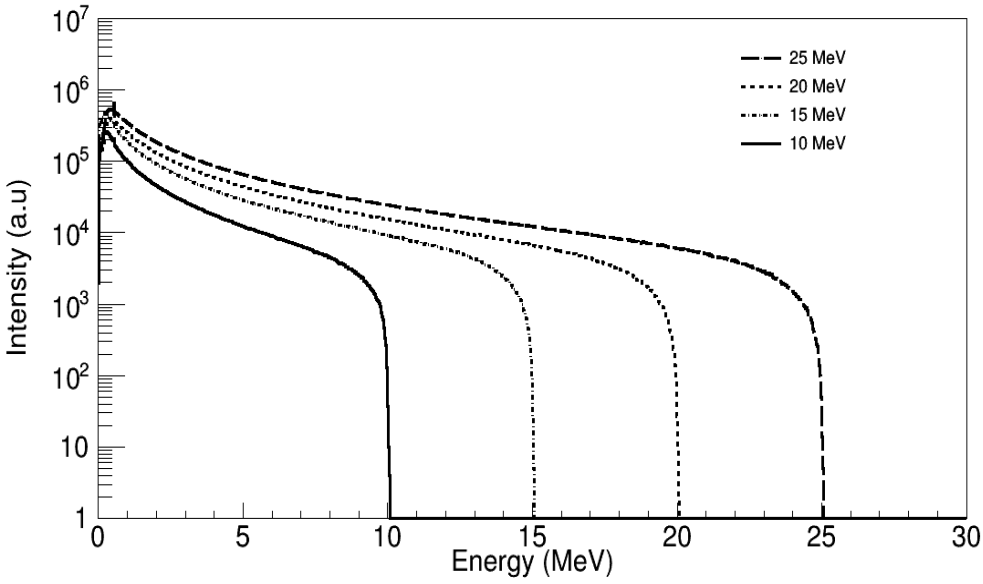

Fig 1. The bremsstrahlung spectra calculated by Geant4.10.06 version.

The thermal neutron source was also created at MT-25 Microtron described in ref. [8]. The uranium-beryllium converter was placed within a graphite cube, which served as a main neutron moderator to thermal and epithermal neutrons.

The high-purity natural Ce_2O_3, PdO, SeO_2 and Cd samples with the mass and diameter of 0.8 g, 0.323 g, 0.2484 g, 0.7143 g and 1.6 cm, 1.0 cm, 1.0 cm, 1.0 cm, respectively were irradiated in the photon and neutron sources with the definite time, which was preliminarily estimated by the activation method so that the interested gamma rays have good count statistics. Afterwards, the gamma-ray activities were measured for proper time of cooling and measurement by using the high-resolution gamma-ray spectroscopy consisting of the high-energy resolution HPGe detector (1.80 keV at γ- ray 1332 keV of ^{60}Co), the PC based 8192 channel analyzers for the data processing, the GENIE 2000 and Gamma Vision software used for the data acquisition and γ-ray spectra analysis [7,8].

3. Data analysis

The selected gamma rays and spectroscopic characteristic data [12,13] used for the IR calculation were determined and shown in Table 1. The losses of the interested gamma ray count due to the self-absorption and summing coincidence effects, which contribute to the IR determination error were corrected as the formulas (1) and (2) in ref. [8].

The IR was calculated below as in refs. [7,8,10]:

$$\frac{1}{IR} = \frac{\dfrac{S_g \varepsilon_m I_m}{S_m \varepsilon_g I_g} \Lambda_3\Lambda_6\Lambda_9 - \Lambda_1\Lambda_5\Lambda_8 - \Lambda_3\Lambda_4\Lambda_8 - \Lambda_3\Lambda_6\Lambda_7}{\Lambda_2\Lambda_5\Lambda_8} \quad (1)$$

Where m and g- the isomeric and ground states; S, ε and I - the counts, the efficiencies and the intensities of the gamma rays of interest and Λ_i (i = 1 ~ 9) are expressions related to the irradiation, cooling and measurement time.

Table 1. Selected gamma rays and spectroscopic characteristic data

Nuclear Reaction	Target Spin, Parity, [J^{π}]	Nuclear state	Spin Parity [J^{π}]	Decay Mode [%]	Half Life	γ-ray Energy [keV]	Intensity [%]
^{138}Ce(γ, n)^{137}Ce ^{136}Ce(n,γ)^{137}Ce	0^+	^{137m}Ce	$11/2^-$	IT: 99.2 EC: 0.78	34.4 h	254.3	99.2
^{138}Ce(γ,n)^{137}Ce ^{136}Ce(n,γ)^{137}Ce	0^+	^{137g}Ce	$3/2^+$	EC: 100	9.0 h	447.1	1.8
^{116}Cd(γ, n)^{115}Cd ^{114}Cd(n, γ)^{115}Cd	0^+	^{115m}Cd	$11/2^-$	β^- : 100	44.6 d	933.8	2.0
^{116}Cd(γ, n)^{115}Cd ^{114}Cd(n, γ)^{115}Cd	0^+	^{115g}Cd	$1/2^+$	β^- : 100	2.23 d	336.2 527.9	45.9 27.45
^{110}Pd(γ,n)^{109,}Pd ^{108}Pd(n,γ)^{109}Pd	0^+	^{109m}Pd	$11/2^-$	IT: 100	4.69 m	189.0	55.9
^{110}Pd(γ,n)^{109}Pd ^{108}Pd(n,γ)^{109}Pd	0^+	^{109g}Pd	$5/2^+$	β^- : 100	13.7 h	88.04	3.6
^{82}Se(γ, n)^{81}Se ^{82}Se(n, γ)^{81}Se	0^+	^{81m,}Se	$7/2^+$	IT: 99.95 β^- : 0.05	57.28 m	103.0	13.0
^{82}Se(γ, n)^{81}Se ^{80}Se(n, γ)^{81}Se	0^+	^{81g,}Se	$1/2^-$	β^- : 100	18.45 m	276.0 290.0	0.7 0.55

4. Results and Discussion

Table 2 presents the experimental results of this work together with the existing data, which were taken from refs. [7,14–23]. The product excitation energies were calcultate by using formula (5) in refs. [8]. The error of IRs came from two sources. The first included uncertainties related to the IR calculations using formula (1) and the second was from uncertainties related to systematics. The total error of the IR determination was estimated to be about 10.0%.

The experimental results show that the IRs in inverse (γ, n) and (n, γ) reactions, which lead to the same isomeric pairs ^{137m,g}Ce, ^{115m,g}Cd, ^{109m,g}Pd, and ^{81m,g}Se are different due to be reaction channel effect. The IRs in (γ, n) reactions are significantly higher than that in (n, γ) reactions. This trend can be explained by the intaken angular momentum and impulse, transferred to the target nuclei from the projectiles, namely the higher the intake angular momentum and impulse the higher the isomeric ratio.

For the (γ, n) reactions, the IRs of this work and that of refs. [15,16,19,22] in the error limit are in good agreement. Likewise, for the (n, γ) reactions, our result and the data from the references are in an agreement except for ^{81m,g}Se to be an agreement with refs. [14,23] and being considerably less than that from ref. [18].

Table 2. The isomeric ratio of the investigated (γ, n) and (n, γ) inverse reactions

Nuclear Reaction and Product	Type of Projectile	Product Exc. Energy [MeV]	Isomeric Ratio *IR*
^{138}Ce(γ, n)^{137m,g}Ce	25 MeV Bremsstrahlung	5.5	0.221(22) (This work) 0.19(2) [16]
^{136}Ce (n, γ)^{137m,g}Ce	Thermal neutron	7.4	0.112(11) (This work) 0.109(10) [7] 0.15(1) [17] 0.088(6) [18]
^{116}Cd(γ, n)^{115m,g}Cd	25 MeV Bremsstrahlung	5.8	0.165(16) (This work) 0.168(20) [19]
^{114}Cd(n, γ)^{115m,g}Cd	Thermal neutron	6.1	0.116(12) (This work) 0.099(33) [20]
^{110}Pd(γ, n)^{109m,g}Pd	25 MeV Bremsstrahlung	6.3	0.069(7) (This work) 0.065(3) [15]
^{108}Pd(n, γ)^{109m,g}Pd	Thermal neutron	6.1	0.023(2) (This work) 0.018(5) [21], 0.028(5) [14]
^{82}Se(γ, n)^{81m,g}Se	25 MeV Bremsstrahlung	6.9	0.556(55) (This work) 0.56(2) [22]
^{80}Se(n, γ)^{81m,g}Se	Thermal neutron	6.7	0.114 ± 0.014 (This work) 0.204(24) [17] 0.136(0.011) [14] 0.096(9) [23]

TALYS 1.95 code [24] and GEANT4 simulation tool were used for theoretical IR calculation of ^{137m,g}Ce, ^{115m,g}Cd, ^{109m,g}Pd, and ^{81m,g}Se produced from (γ, n) reaction. TALYS code simulates nuclear reactions that involve neutrons, gamma-rays, protons, deuterons, tritons, helions, and alpha-particles in the 1 keV–200 MeV energy range. In the thermal energy region of neutron, this code is completely unresolved. In case of bremsstrahlung induced nuclear reactions, the isomeric ratios could be analytically calculated by the expression below:

$$IR = \frac{Y_m}{Y_g} = \frac{N_0 \int_{E_{th}^m}^{E_\gamma^m} \sigma_m(E)\phi(E)dE}{N_0 \int_{E_{th}^g}^{E_\gamma^m} \sigma_g(E)\phi(E)dE}. \quad (2)$$

Here E_g^m - the bremsstrahlung end-point energy, ϕ (E) – the bremsstrahlung photon flux, N_0 - the number of the target nuclei; $\sigma_m(E)$ and $\sigma_g(E)$ - the cross sections of the isomeric and ground states; E_{th}^m and E_{th}^g - the threshold reaction energies for the isomeric and ground state, respectively.

By using the TALYS 1.95 code, $\sigma_m(E)$ and $\sigma_g(E)$ could be obtained. These data combining with the bremsstrahlung spectra simulated by GEANT4 (Fig. 1) could be caculated IR following the formula (2). The theoretical IR results were obtained by the calculation using six level density models of TALYS 1.95 as ldmodel 1: Constant temperature + Fermi gas model; ldmodel 2: Back-shifted Fermi gas model; ldmodel 3: Generalised superfluid model; ldmodel 4: Microscopic level densities (Skyrme force) from Goriely's tables; ldmodel 5: Microscopic level densities (Skyrme force) from Hilaire's combinatorial tables and ldmodel 6: Microscopic level densities (temperature dependent HFB, Gogny force) from Hilaire's combinatorial tables. The present experimental results are best suited to the predictions using the 6th level density model. The deviations between the experimental and calculated data using 6 level density models are less than 23% (see Fig. 2) except for ^{137m,g}Ce. The difference in the case of ^{137m,g}Ce requires the level density and strength function models to be more detailed.

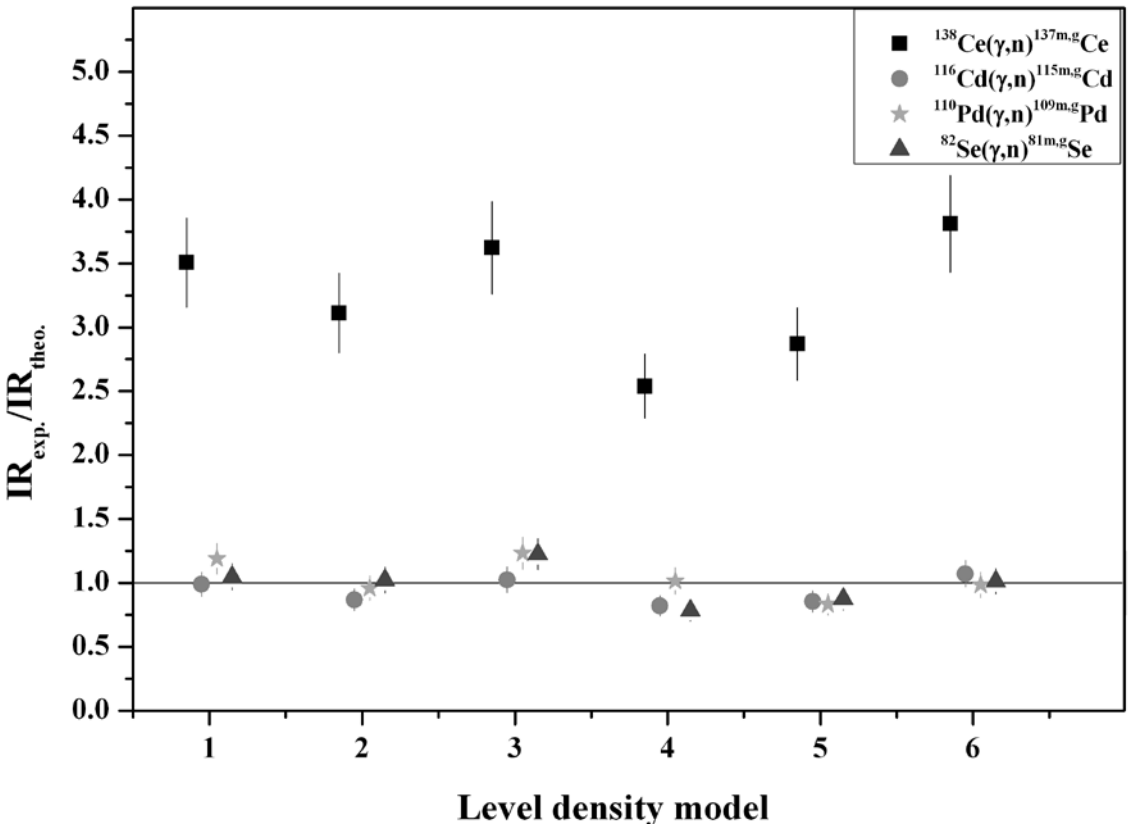

Fig. 2. Measured ($IR_{exp.}$) and calculated ($IR_{theo.}$) isomeric ratios of ^{137m,g}Ce, ^{115m,g}Cd, ^{109m,g}Pd and ^{81m,g}Se produced by (γ, n) reaction.

5. Conclusions

The IRs of ^{137m,g}Ce, ^{115m,g}Cd, ^{109m,g}Pd and ^{81m,g}Se in inverse (γ, n) and (n, γ) reactions have been measured by the activation method. The experimental results show that the IRs in (γ, n) reaction are higher than that in (n, γ) reaction. This trend can be explained by the effects of reaction channel, intaken angular momentum and impulse in nuclear reation.

The theoretical calculations for (γ, n) reactions based on TALYS 1.95 code are consistent with the experimental results, except in the case of ^{138}Ce(γ, n)^{137m,g}Ce reaction.

In order to reach a complete conclusion, it is needed more experiments to be performed as well as a nuclear reaction model, which includes detailed nuclear structure and nuclear reaction mechanisms as the compound, preequilibrium and direct.

Acknowledgment

This work has been performed at the Flerov Laboratory of Nuclear Reaction, Joint Institute for Nuclear Research, Dubna, Russia. The authors would like to express sincere thanks to the MT-25 Microtron group for operating the irradiation facility and the Chemical Department of the Flerov Laboratory of Nuclear Reaction for providing the measurement system. Bui Minh Hue was funded by Vingroup Joint Stock Company and supported by the Domestic PhD Scholarship Program of Vingroup Innovation Foundation (VINIF), Vingroup Big Data Institute (VINBIGDATA), code VINIF.2020.TS.18.

References

1. Cohen, S.G., Fisher, P.S. and Warburton E.K., 1961. Inverse Photonuclear Reactions ^{14}N(p, γ)^{14}O and ^{15}N(p, γ)^{16}O in the Giant Resonance Region. Phys. Rev. **121**(3), 858–865.
2. Wahsweiler H.G. and Greiner W. 1967. Angular distributions for the inverse photonuclear process in Si28 in the eigenchannel reaction theory. Phys. Rev. Lett. V. **19**(3), 131–134.
3. Mohr P., Angulo C., Descouvemont P. and H., 2006. Relation between the ^{16}O(α, γ)^{20}Ne reaction and its reverse ^{20}Ne(γ, α)^{16}O reaction in stars and in the laboratory, Eur. Phys. J. A **27**(1), 75–78.
4. Beard M., Frauendorf S., Kampfer B., Schwengner R. and Wiescher M., 2012. Photonuclear and radiative-capture reaction rates for nuclear astrophysics and transmutation: $^{92\text{-}100}$Mo, ^{88}Sr, ^{90}Zr, and ^{139}La. Phys. Rev. C **85**, 065808.
5. Huizenga J.R. and Vandenbosch R., 1960. Interpretation of Isomeric Cross Section Ratios for (n, γ) and (γ, n) Reactions. Phys. Rev. **120**(4), 1305–1312.
6. Do N.V., Luan N.T., Xuan N.T., Khue P.D., Hien N.T., Kim G., Kim K., Shin S.G., Kye Y., Cho M.H., 2020. Measurement of yield ratios for the isomeric pair ^{137m,g}Ce in the ^{141}Pr(γ, x)^{137m,g}Ce reactions with bremsstrahlung end-point energies of 50-, 60-, and 70-MeV. Radiation Physics and Chemistry, **176**, 1–9, 10901.
7. Thiep T.D., An T.T., Cuong P.V., Vinh N.T., Hue B.M., Belov A.G., Maslov O.D., 2017. Channel effect in isomeric ratio of ^{137m,g}Ce produced in different nuclear reactions. J. Radioanal. Nucl. Chem., **314**, 1777–1784.
8. Hue B.M., Thiep T.D., An T.T., Cuong P.V., Lukyanov S.M., Belov A.G., Mitrofanov S., 2020. The isomeric ratios in (n, γ) neutron capture reactions on ^{108}Pd and ^{110}Pd nuclei, J. Radioanal. Nucl. Chem., **326**(1), 503–509.
9. Belov A.G., Bondarenko P.G., Teteriev Yu.G. 1993. Preprint of JINR, D15-93-80, Dubna, Russia.
10. Thiep T.D., An T.T, Cuong P.V., Vinh N.T., Hue B.M., Anh L.T., Belov A.G., 2018. Isomeric Yield Ratio of ^{152m1}Eu(8-) to ^{152m2}Eu(0-) Produced from ^{153}Eu (γ, n)^{152}Eu Reaction in the Giant Dipole Resonance Region, J. Radioanal. Nucl. Chem., **317**, 1263–1271.

11. Geant4 Collaboration, Physics Reference Manual, Release 10.4, 2017.
12. Firestone R.B. 1996. Table of Isotopes, CD ROM Edn., Version 1.0, Wiley-Interscience, New York.
13. Radiation Search, http://ie.lbl.gov/toi/radSearch.asp53.
14. Bishop C.T., Vonach H.K. and Vandenbosch R.,1964. Isomer Ratio for Some (n, γ) Reactions. Nucl. Phys. A **60**, 241–249.
15. Palvanov S.R., Bozorov E.K., Mamajusupova M.I., Palvanova G.S., Saidimov Y.A., 2017. Excitation of Isomeric States in Reactions (γ, n) and (n, 2n) on ^{110}Pd Nucleus. World Journal of Research and Review, **5**(5), 28–31.
16. Gangrsky Yu.P., Zuzaan P., Kolesnikov N.N., Lukashek V.G., Tonchev A.P., 2001. Isomeric Ratios in Crossing (n, γ) and (γ, n) Reactions. Bull. Rus. Acad. Sci. Phys. **65**, 121–126.
17. Bernard K. 1963. Yield ratios of isomers produced by neutron activation. Phys. Rev. **129**(2), 769–775.
18. Torrel S. and Krane K.S., 2012. Neutron capture cross sections of ^{136,138,140,142} Ce and the decays of ^{137}Ce, Phys Rev. C **86**: 034340.
19. Kyryjenko A.V., Osipenko A.P., Parlag A.M., Pylypchenko V.A., Sabolchiy N.T., Sokolyuk I.V., Khimich I.V., 2006. Investigation of the cadmium nuclei isomers state excitation in the photonuclear reactions. Uzhgorod University Scientific Herald, Series Physics 19, 85–89.
20. Gicking A.M., Takahashi K., Krane K.S., 2019. Neutron capture cross sections of stable Cd isotopes, Eur. Phys. J. A **55**, 52–62.
21. Sehgal M.L., Hans H.S., Gill P.S., 1959. Thermal neutron cross-sections for producing some isomers, Nucl. Phys. **12**(3), 261–268.
22. Palvanov S., 2018. Cross Section of Excitation of Isomer States 81m,gSe in the Reaction (γ, n) and (n, 2n), Journal of Scientific and Engineering Research. **5**(1), 41–45.
23. Nakamura S., Furutaka K., Harada H., Katoh T., 2008. Thermal-Neutron Capture Cross Sections and Resonance Integrals of the ^{80}Se(n,γ)^{81m,g}Se Reaction. Journal of Nuclear Science and Technology **45**(2), 116–122.
24. Koning A.J. and Rochman D., 2012. Modern Nuclear Data Evaluation with the TALYS Code System, NUCLEAR DATA SHEETS, TALYS 1.8, p. 1–94. See also on: www.talys.eu.